

Novel Technique for Locating an Intruder in 3D Environments by Using a Cooperative System of Multistatic Radars

Josivaldo de S. Araújo, Rodrigo M. S. de Oliveira and Carlos Leonidas da S. S. Sobrinho
Universidade Federal do Pará (UFPA) - ICEN & ITEC - josivaldo@ufpa.br, rmso@ufpa.br, leonidas@ufpa.br

Abstract— the aim of this work is to present a new methodology, based on vector and geometrical techniques, for determining the position of an intruder in a residence (3D problem). Initially, modifications in the electromagnetic responses of the environment, caused by movements of the trespasser, are detected. It is worth mentioning that slight movements are detected by high frequency components of the used pulse. The differences between the signals (before and after any movement) are used to define a sphere and ellipsoids, which are used for estimating the position of the invader. In this work, multiple radars are used in a cooperative manner. The multiple estimates obtained are used to determine a mean position and its standard deviation, introducing the concept of sphere of estimates. The electromagnetic simulations were performed by using the FDTD method. Results were obtained for single and double floor residences.

Index Terms— Pinpointing of intruder's position, vector technique, multistatic radar, monopole antenna, dipole antenna, indoor sensors, double-floor residence.

I. INTRODUCTION

Considerable increase of the attention of researchers to indoor radar systems has been observed in last decade [1-4]. This kind of system is able to detect and precisely locate intruders, even when they are positioned among walls and furniture. These radars use UltraWideBand (UWB) pulses [1] for detecting the presence of an intruder by measuring differences on electromagnetic responses when these pulses are propagated at different moments. These pulses are extremely narrow in time, what characterizes them as ultrawideband signals. This characteristic provides to the pulse enhanced immunity to selective attenuations of frequencies, which are inherent to scattering environments. Due to the fact that the UWB pulses are so narrow, they can use broad frequency spectra, allowing the signals to use low power, what minimizes the interference with other communication systems, such as cell phones, GPS, Bluetooth, W-LAN IEEE 802.11, among others [2].

The finite-difference time-domain method (FDTD), developed by Kane Yee [5], when applied to solve Maxwell's equations, allows the simulation of the propagation of electromagnetic waves in time domain, providing full-wave solutions. In this work, this technique was combined to the *Uniaxial*

Perfectly Matched Layer (UPML) formulation [6], in order to truncate the analysis region. In this way, this technique simulates an anechoic chamber.

Based on the ideas discussed above, the aim of this work is to present a methodology which estimates the position of an intruder in a tridimensional environment through detecting modifications in the transient responses of the environment about wideband (WB) pulses, caused by the movements of the intruder. Even if these movements are slight, the detection is possible due to the higher frequency components of the pulse. The estimate of the position will be held through a vector technique proposed in this work. This paper represents advance to previous works, because, besides approaching the problem in 3D, when previous works are limited to the 2D case [3,4], it introduces a simpler methodology. The power spectrum of the used wideband pulse ranges from 0.3 to 0.8 GHz. It is observed in this paper that pulses in this frequency range, associated to the developed methodology, can be used for properly estimate the intruder's position inside an ordinary indoor environment. The developed methodology was tested by using data obtained from the full-wave numerical simulations.

II. ENVIRONMENT DESCRIPTION AND SIMULATION PARAMETERS

In this work, tridimensional indoor environments are considered. Fig.1 illustrates the first scenario simulated. In this environment, there are two distinct kinds of walls, characterized by different electrical parameters, which are: the relative electric permittivity of external walls is $\epsilon_r = 5.0$ and, for those of the interior, $\epsilon_r = 4.2$. The used conductivity is $\sigma = 0.02$ S/m for every wall [7]. Everywhere else, the relative permittivity is equal to unity and $\sigma = 0$, except in the ground region, which penetrates the UPML. The thickness of walls is 30 (external) and 18 (internal) centimeters [7]. Every media is modeled by using $\mu = \mu_0$.

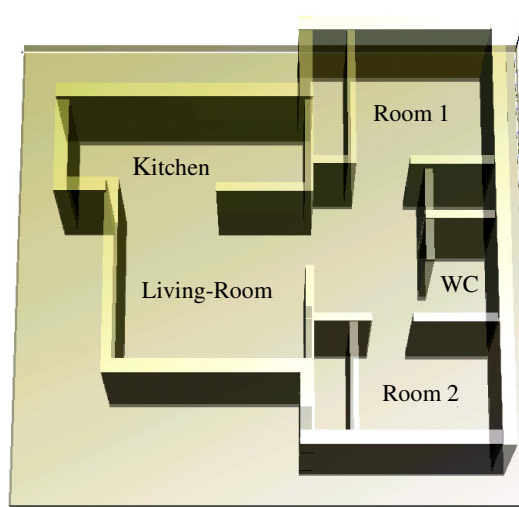


Fig.1. The single-floor residence layout.

The simulations are performed by using the 3D-FDTD method for nondispersive isotropic media (analysis region), based on the Yee's formulation [5]. Here, a mesh with $384 \times 352 \times 120$ cells was used. Cubic Yee's cells with $\Delta s = 3.0$ cm ($\Delta s = \Delta x = \Delta y = \Delta z$) were used. Δs is equivalent to approximately one-tenth of the minimum free-space wavelength of the excitation pulse, in order to reduce numerical dispersion effects. The time increment Δt was obtained from Δs , in order to assure the numerical stability of the method. In this paper, 70% of the Courant's limit is used [6-8]. The parameters of the UPML were optimized in order to reduce undesired reflections: thickness of 10 cells, maximum attenuation conductivity $\sigma_{\max} = 15$ S/m, and the order of the attenuation polynomial function is $m = 4$. Here, a Beowulf cluster with 16 cores was used for generating the transient signals.

The waveform used as an excitation source, in order to scan the environment, is the Gaussian monocycle pulse. This type of pulse is used, for example, by the PulsON system [9].

The Gaussian monocycle is the first derivative of Gaussian function with respect to time, which is given by

$$p(t) = -A_p \sqrt{\frac{2e}{\tau^2}} (t - t_0) \exp \left[-\frac{(t - t_0)^2}{\tau^2} \right], \quad (1)$$

where $e \approx 2.71828$, $A_p = 1$ V/m, $\tau = 0.255$ ns and $t_0 = 1.8$ ns. This function is plotted in Fig.2.

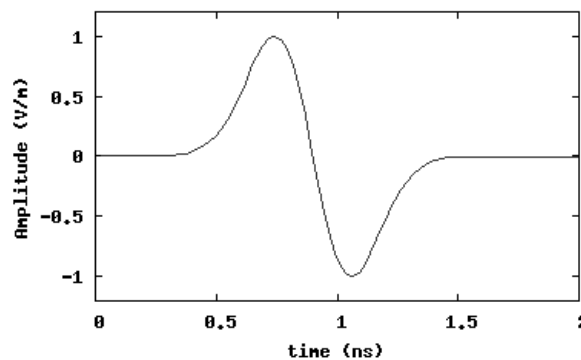


Fig.2 – Graphical representation of the wideband excitation pulse (time domain).

In order to complete the environment description, the only missing item is the target. In order to represent the intruder, it was used the model presented in Fig.3, with approximately 1.70 m in height. The relative permittivity considered for the intruder is $\epsilon_r = 50$ and its conductivity is $\sigma = 1.43$ S/m [10], which represent average parameters.

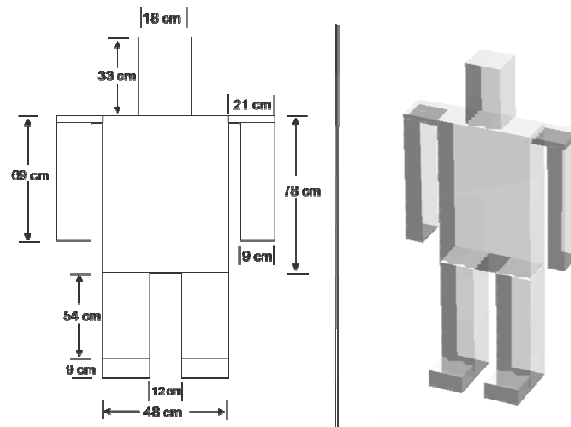


Fig.3. Representation of the human being (intruder).

One of the transceiver antennas used for this work is a wideband dipole with the dimensions defined in Fig.4. The antenna dimensions are $c = 12$ cm, $w = 6$ cm, $h = 6$ cm and $d = p = 3$ cm. The rod radius is 7,5 mm, modeled by thin wire [11]. This dipole's bandwidth is approximately 300 MHz for 50Ω feeding impedance.

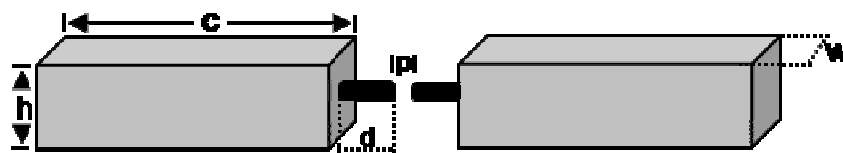


Fig.4. Diagram of the dipole antenna used as transceiver.

The radar system was also simulated by using the monopole antenna shown by Fig.5. It consists on a cuboid conductor, with dimensions $h = 9$ cm, $w = c = 6$ cm and $d = 3$ cm, with $p = 30$ cm. The distance from the ground plane to the vertical rectangular radiator is 3 cm. This monopole's bandwidth is approximately 500 MHz (50Ω feeding impedance).

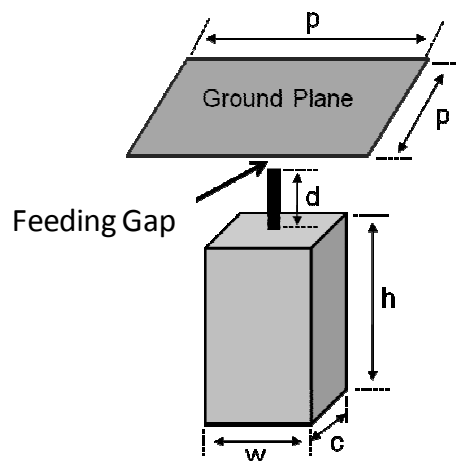


Fig.5. Diagram of the monopole antenna used as transceiver.

III. RADAR APPLICATION

In order to determine the position of the intruder in the simulated environment, for the case of the residence presented in Fig.1 (by using the origin of the system of coordinates as reference), two mathematical methods were used: the FDTD method, for generating electromagnetic field data; and the concept of propagating ray [8,12], for obtaining the parameters of the sphere and ellipsoids used for localization. When a two dimensional case is analyzed, two aspects related to propagating rays are considered: 1) the transceiver antenna transmits the pulse, which reflects at the target and returns to the transceiver. The time the wave needs to complete this path is used to define a circumference, centered at the transceiver, in which the trespasser may be positioned on any of its points. 2) the transceiver transmits the pulse, which reflects at the intruder and reaches a receiver. The time the signal needs to complete this path is used to define an ellipse, in which the trespasser may be positioned on any of its points [7]. The second case is also valid for other receivers. This defines a system of equations which solution is an estimate of the position of the undesired visitor. If the wave propagates in free space, the system's solution is the exact position of the man, as long as the propagating speed would be that of free space, everywhere. When three-dimensions are considered, this idea is still valid. However, a sphere and ellipsoids must be considered.

The cooperative system used to determine the position of the intruder is presented by Fig.6, where four transceiver antennas can be observed, numbered from 1 to 4, as well as their positions in space. The system works as a cooperative multistatic radar. It is also observed from Fig.6 that there are two *x*-polarized (transceiver) dipoles and two *y*-polarized dipoles (for the cooperative system based on the dipole antenna). The goal is to avoid that the intruder gets to be simultaneously positioned at a null of two or more (transceiver) antennas' radiating patterns, what could make the pinpointing of the position difficult. A system based on *z*-polarized cuboid monopole antennas (Fig.5) was also tested.

In order to determine the position of the intruder, the wideband pulse defined by (1) is transmitted. Then, the temporal evolution of the electric field is registered in several points (receivers) and stored as reference. The pulse is then retransmitted and the transient electric field is once more registered by the receivers. Any movement performed by the intruder inside the house, as for example, a little movement of his head distorts the signals captured, which are compared to the transient responses previously obtained. After processing these data, the radii of the ellipsoids (each with foci positioned at a transceiver and a receiver positions) and the radii of spheres (each centered at a transceiver's position) [3] are obtained.

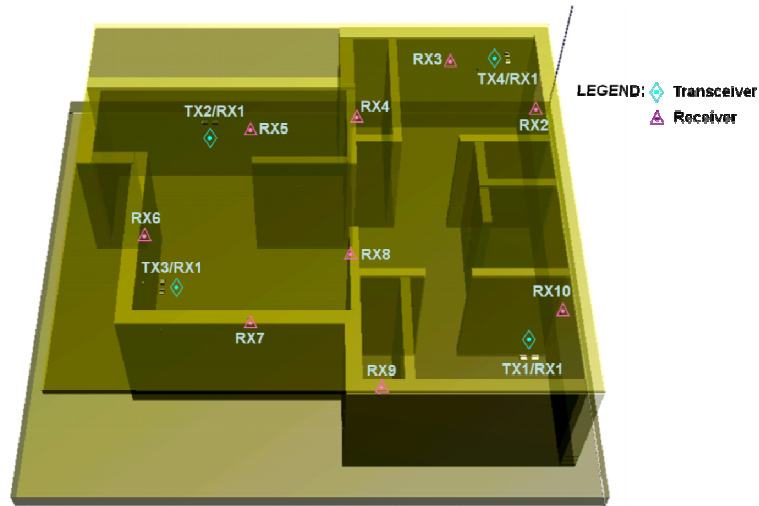


Fig.6. Representation of the Environment of Simulation and Position of the Transceiver Antennas.

A transceiver and two receivers define a multistatic radar system, which produces an estimation of the position of the intruder. This way, the combination of this transceiver with other pair of receivers produces a different estimate, as it also happens when other transceiver is considered. In this case, several estimates are computed and a statistic analysis is performed. For each transceiver, the mean position and its standard deviation are calculated, and a *sphere of estimates* (centered at the mean position with radius identical to the calculated standard deviation) is defined. This sphere encloses a region of space in which the intruder is possibly positioned when that transceiver is considered. This way, four spheres of estimates are determined. In order to decide which transceiver produces more reliable estimates, the smaller radius (standard deviation) sphere is considered.

IV. THE PROPOSED METHODOLOGY

Consider a vector \overline{AB} oriented from point A (x_A, y_A, z_A) to point B (x_B, y_B, z_B), such as indicated by Fig.7. Point A defines the position of a transceiver and point B defines the position of a receiver. Vector $\overline{AB} = \vec{x}$ can be written as

$$\vec{x} = (x_B - x_A, y_B - y_A, z_B - z_A) = (x_x, x_y, x_z). \quad (2)$$

In (2), x_x, x_y and x_z , which are defined for sake of simplicity, are, this way, given by

$$\begin{cases} x_x = x_B - x_A \\ x_y = y_B - y_A \\ x_z = z_B - z_A. \end{cases} \quad (3)$$

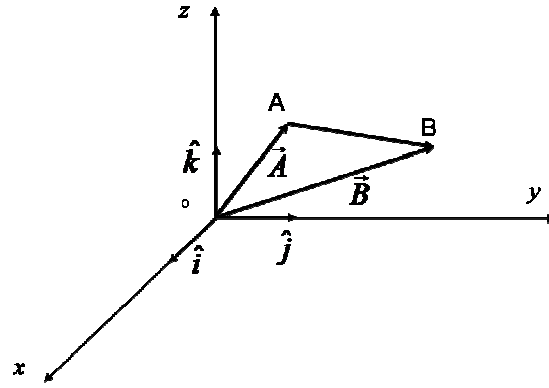


Fig.7.: The vector \vec{AB} pointing from the transceiver point A to a receiver point B.

Consider a point P positioned anywhere in the space, except the line containing A and B. The unit vectors of \vec{P} (\hat{x}_p, \hat{y}_p and \hat{z}_p) can be calculated by

$$\hat{x}_p = \frac{x_p}{|\vec{P}|} \hat{i}; \quad \hat{y}_p = \frac{y_p}{|\vec{P}|} \hat{j}; \quad \hat{z}_p = \frac{z_p}{|\vec{P}|} \hat{k}, \quad (4)$$

where

$$|\vec{P}| = \sqrt{x_p^2 + y_p^2 + z_p^2}. \quad (5)$$

In (4) and (5), x_p, y_p and z_p are the coordinates of P. The points A, B and P are used to define a second coordinate system, which has its x', y' and z' axes aligned to the following directions:

a) direction \hat{i}' : it is defined as the unit vector directed from A to B (which represent the foci of a ellipse placed in 3D space). It is obtained from vector \vec{x}' (given by (2)). This way, \hat{i}' is given by

$$\hat{i}' = \frac{\vec{x}'}{|\vec{x}'|}; \quad (6)$$

b) direction \hat{j}' : it is the unit vector parallel to \vec{y}' , which is given by the cross product of the vectors \vec{x}' and \vec{P} . Thus, \vec{y}' is calculated by

$$\vec{y}' = \begin{vmatrix} \hat{i} & \hat{j} & \hat{k} \\ x_p & y_p & z_p \\ x_x & x_y & x_z \end{vmatrix}, \quad (7)$$

resulting in a vector normal to \vec{x}' given by

$$\vec{y}' = \underbrace{(x_z y_p - z_p x_y)}_{y_x} \hat{i} + \underbrace{(x_x x_p - z_p x_x)}_{y_y} \hat{j} + \underbrace{(x_p x_y - x_x y_p)}_{y_z} \hat{k}. \quad (8)$$

Finally, the unit vector \hat{j}' is calculated by

$$\hat{j}' = \frac{\vec{y}'}{|\vec{y}'|} \tag{9}$$

c) direction \hat{k}' : After defining the directions \hat{i}' and \hat{j}' , it is calculated a cross product for determining a vector \vec{z}' . As long as \vec{z}' must be orthogonal to both \vec{x}' and \vec{y}' , we have

$$\vec{z}' = \vec{x}' \times \vec{y}' = \begin{vmatrix} \hat{i}' & \hat{j}' & \hat{k}' \\ x_x & x_y & x_z \\ y_x & y_y & y_z \end{vmatrix} \tag{10}$$

or

$$\vec{z}' = \underbrace{(x_y y_z - x_z y_y)}_{z_x} \hat{i}' + \underbrace{(x_x y_z - x_z y_x)}_{z_y} \hat{j}' + \underbrace{(x_x y_y - x_y y_x)}_{z_z} \hat{k}' \tag{11}$$

Finally, the unit vector \hat{k}' is obtained by using (12), as follows

$$\hat{k}' = \frac{\vec{z}'}{|\vec{z}'|} \tag{12}$$

In order to perform the transformation of coordinates around the origin, by using the former coordinate system as reference, the equation

$$\begin{bmatrix} x_r \\ y_r \\ z_r \end{bmatrix} = \begin{bmatrix} l_1 & l_2 & l_3 \\ m_1 & m_2 & m_3 \\ n_1 & n_2 & n_3 \end{bmatrix} \begin{bmatrix} x \\ y \\ z \end{bmatrix} \tag{13}$$

is solved, in which $(l_1, m_1, n_1, l_2, m_2, n_2, l_3, m_3, n_3)$ are the direction cosines related to x, y and z , respectively. From (13), the equations

$$\begin{aligned} x_r &= l_1 x + l_2 y + l_3 z, \\ y_r &= m_1 x + m_2 y + m_3 z, \end{aligned} \tag{14}$$

and

$$z_r = n_1 x + n_2 y + n_3 z,$$

are obtained, in which the direction cosines are given by

$$\begin{aligned} l_1 &= \hat{i}' \cdot \hat{i}' \quad ; \quad l_2 = \hat{j}' \cdot \hat{i}' \quad ; \quad l_3 = \hat{k}' \cdot \hat{i}' ; \\ m_1 &= \hat{i}' \cdot \hat{j}' \quad ; \quad m_2 = \hat{j}' \cdot \hat{j}' \quad ; \quad m_3 = \hat{k}' \cdot \hat{j}' ; \\ n_1 &= \hat{i}' \cdot \hat{k}' \quad ; \quad n_2 = \hat{j}' \cdot \hat{k}' \quad ; \quad n_3 = \hat{k}' \cdot \hat{k}' . \end{aligned} \tag{15}$$

After performing the transformation of coordinates, it is necessary to rotate the ellipse, so that points of an ellipsoid (aligned to \hat{i}') are calculated. In a general way, an arbitrary unit vector $\vec{L}=(l_x, l_y, l_z)$ is used to define rotation. The coordinates x_R, y_R and z_R , obtained by performing the rotation of (x, y, z) around \vec{L} by an angle α , are given by

$$\begin{bmatrix} x_R \\ y_R \\ z_R \end{bmatrix} = [R] \begin{bmatrix} x \\ y \\ z \end{bmatrix} = \begin{bmatrix} l_x^2 + (1-l_x^2)c & l_x l_y (1-c) - l_z s & l_x l_z (1-c) + l_y s \\ l_x l_y (1-c) + l_z s & l_y^2 + (1-l_y^2)c & l_y l_z (1-c) - l_x s \\ l_x l_z (1-c) - l_y s & l_y l_z (1-c) + l_x s & l_z^2 + (1-l_z^2)c \end{bmatrix} \begin{bmatrix} x \\ y \\ z \end{bmatrix}, \quad (16)$$

in which $[R]$ is the rotation matrix, $c = \cos(\alpha)$ and $s = \sin(\alpha)$.

In order to obtain the rotation around the axis x' , (17) is used in (16).

$$l_x = \frac{x_x}{|\vec{x}'|}, \quad l_y = \frac{x_y}{|\vec{x}'|}, \quad l_z = \frac{x_z}{|\vec{x}'|}. \quad (17)$$

It is noticed that (17) satisfies (18), which is a required condition.

$$l_x^2 + l_y^2 + l_z^2 = 1. \quad (18)$$

In synthesis: a) initially one generates a ellipse (Fig.8a) on the coordinate system of reference (x,y,z) (the radii of the ellipse are obtained by using the difference of the transient signals obtained at the associated receiver [3] and $z=0$); b) one defines a new coordinate system by using (2)-(12) and performs the transformation of coordinates around the origin by using (13)-(15) (Fig.8b); c) ellipse in 3D space is then rotated by using (16)-(19), generating this way the corresponding ellipsoid (Fig.8c); d) finally, the multistatic radar's geometry is defined by considering a transceiver (sphere) and two receivers (Fig.8d). The estimate of the trespasser's position is defined by the point equidistant to the three surfaces, such as it is illustrated by Fig.8d.

V. RESULTS

In order to pinpoint the intruder's position, nine receivers and four transceiver dipole antennas were set up in different parts of the house (Fig.6). The cooperative multistatic system was tested for four different cases. For the first and second cases, a single-floor residence is considered and the intruder was positioned at different rooms. His head was displaced by a single Yee's cell. For the third case, the intruder moves one of his legs. Finally, it is considered a double-floor residence in the fourth case.

For the first case (Fig.9), the center of the head of the intruder is located at $x = 2.48$ m, $y = 2.53$ m, $z = 1.70$ m and the intruder is located at bedroom 1. The sphere of estimates (which encloses the region of space with higher probability of finding the man), depicted in Fig.9, is fully contained in the room where the intruder is located. It was obtained by using the system shown in Fig.6. A sphere of estimates was determined for each transmission antenna. The region enclosed by the sphere with the smaller radius (estimate with the less significant standard deviation) was considered to be the radar's estimate (Table I). This sphere is represented in Fig.9 and it is clearly seen that the intruder's head is inside the estimated region.

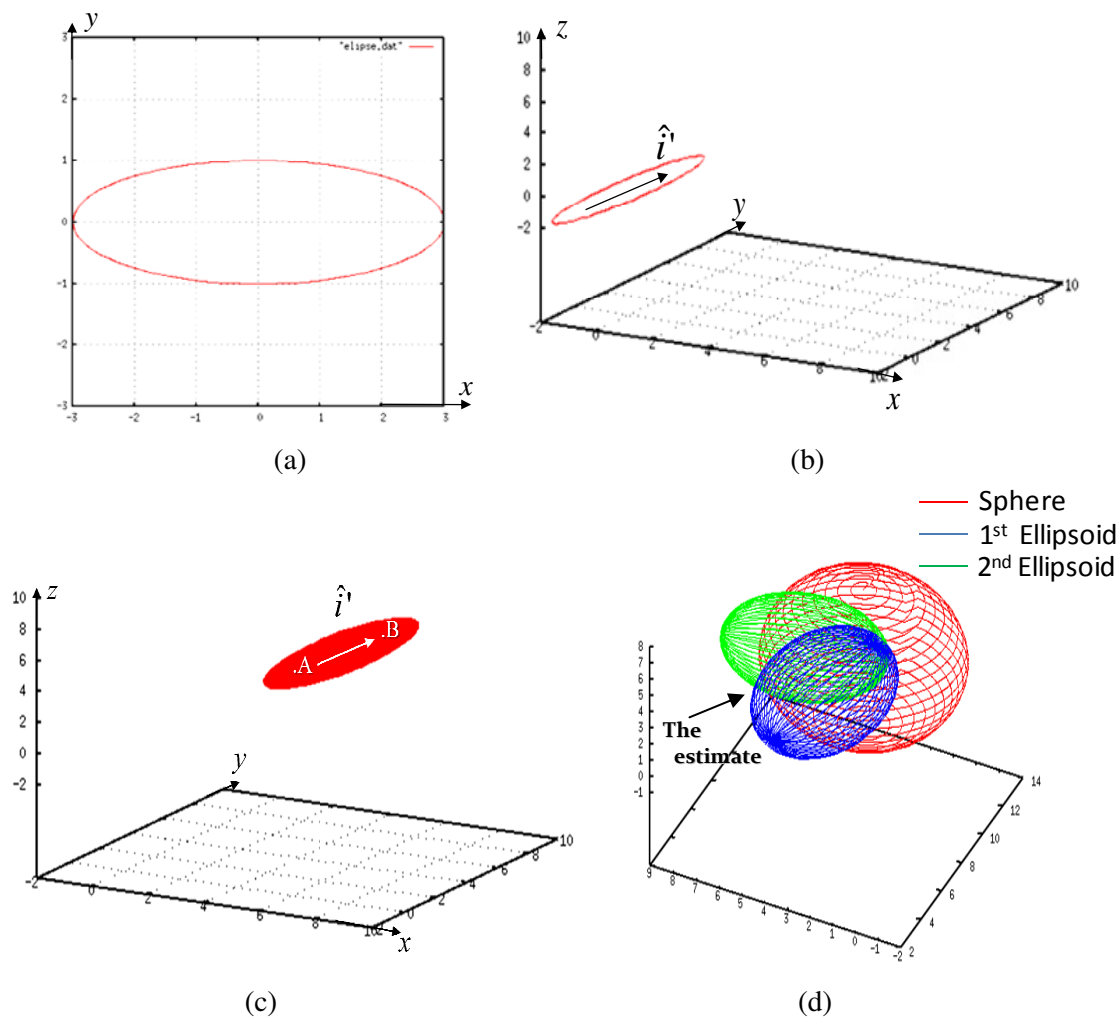


Fig. 8. Steps necessary for defining the multistatic radar's geometry: (a) a ellipse on the xy -plane, (b) transformation of coordinates (ellipse in 3D space), (c) rotation of the ellipse around \hat{i} and translation of coordinates for aligning the ellipsoid to \overline{AB} and (d) the multistatic radar's geometry (considering a transceiver associated to the sphere and two receivers associated to the ellipsoids).

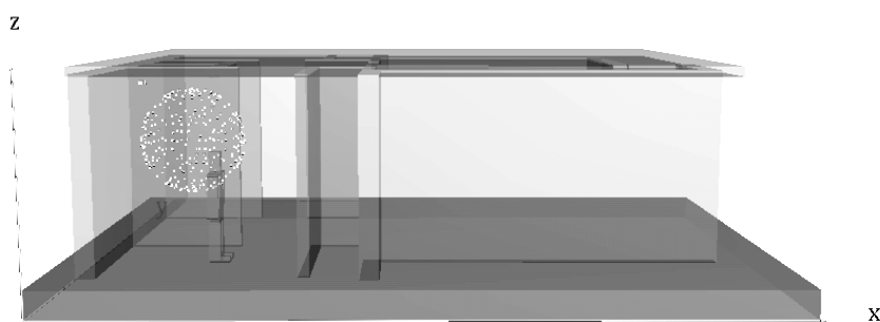


Fig.9. Side view (x - z plane) of the the intruder in bedroom 1 and a sphere of estimates. Movement of head was considered.

As it has been described in section III, the electromagnetic pulse is transmitted twice (after a certain period of time), in such way that movements of the person can be detected by the system. The detection is performed by computing the point to point difference between the two signals obtained at the receivers and at the transceiver points. For two different receivers, both signals received are plotted in Figs.10a and 10b.

TABLE I. SPHERES OF ESTIMATES' RADII (FIRST CASE).

Transceiver	Dipole Antenna		Monopole Antenna	
	Radius (meters)	Radius (cells)	Radius (meters)	Radius (cells)
TX1/RX1	1.53	51	1.35	45
TX2/RX1	1.47	49	1.62	54
TX3/RX1	1.77	59	1.47	49
TX4/RX1	0.81	27	0.66	22

As it can be seen in Fig.10, there is a slight difference between the signals. This small discrepancy is due to the fact that the intruder performed a minor movement (of 3 cm) of his head. Despite this slight difference between the signatures, the system is able to properly locate the intruder.

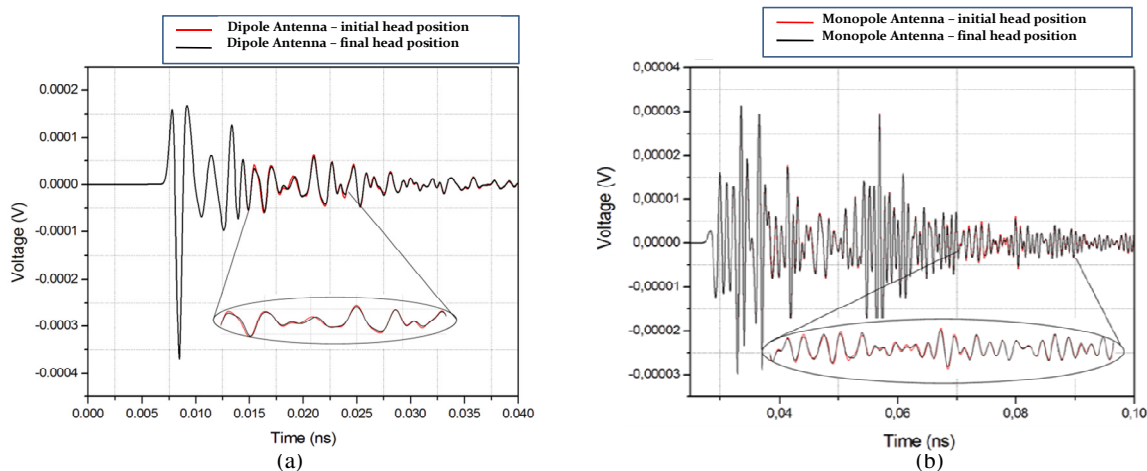


Fig.10. Signatures obtained at two receivers considering the initial and final positions of the intruder's head. In (a) Dipole Antenna and (b) Monopole Antenna.

For the second case (Fig.11), the trespasser is at the kitchen. In this case, the intruder is placed near to TX2 (Fig.6). The head of the intruder is centered at $x = 6.08$ m, $y = 3.44$ m, $z = 1.70$ m. In Fig.11, a side view (x - z plane) of the intruder placed in the kitchen is presented. The sphere of estimates depicted in Fig. 11 (the sphere with the shortest radius) correctly indicates the room where the intruder is located. The information related to the spheres of estimates, for this case, is available in Table II.

TABLE II. ESTIMATIVE SPHERE'S RADIUS RELATIVE TO EACH TRANSCEIVER (SECOND CASE).

Transceiver	Dipole		Monopole	
	Radius (meters)	Radius (cells)	Radius (meters)	Radius (cells)
TX1/RX1	0.84	28	1.11	37
TX2/RX1	0.51	17	1.05	35
TX3/RX1	1.50	50	1.38	46
TX4/RX1	0.57	19	1.17	39

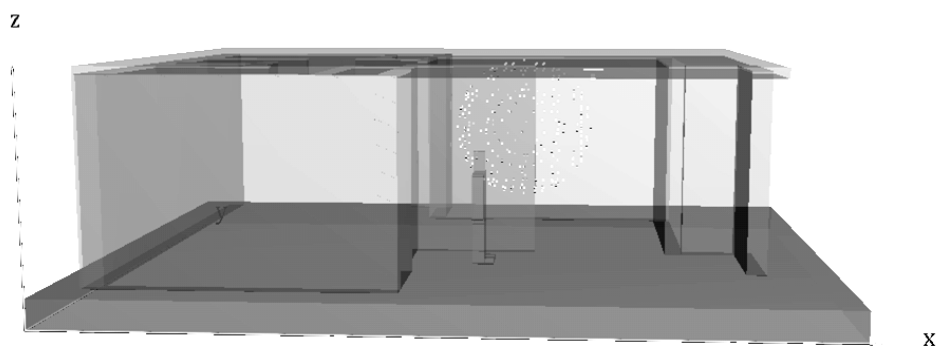


Fig.11. Side View (x - z plane) of the the intruder in the kitchen and a sphere of estimates. Movement of head was considered.

In the third case, the intruder is placed at bedroom 1 and the center of one of his legs is located at the position $x= 2.50$ m, $y = 2.30$ m, $z = 0.78$ m. In Fig.12a, one has a side view (x - z plane) of the intruder in the bedroom 1 and the associated estimative sphere. Fig 12b shows the intruder's leg at its new position, after performing the movement. The sphere defines the room where the intruder is located. Again, in order to determine the position of the intruder, the sphere with the shortest radius was considered, as it can be seen in Table III. Once more, TX4 produced the smallest statistical deviation, as in the first case. It can be observed by comparing Figs. 9 and 12a that the sphere of estimates of the third case was formed closer to the men's leg, implying in consistency of the presented methodology.

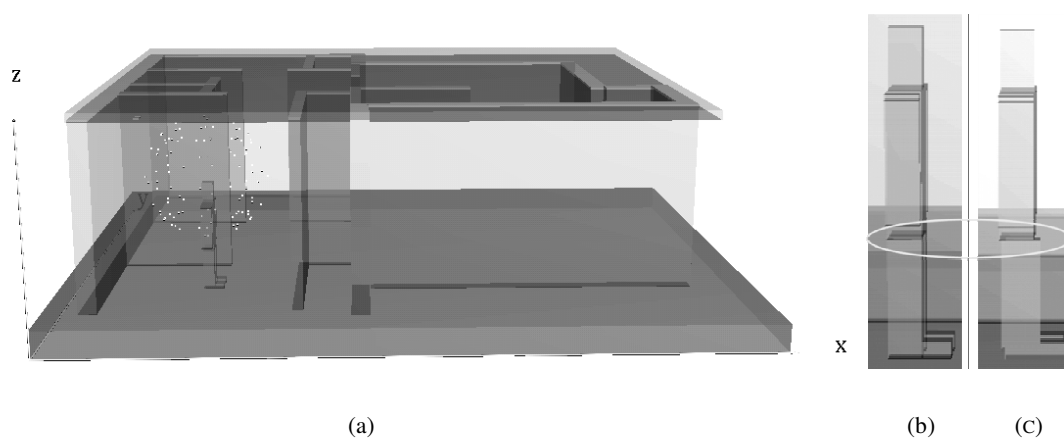


Fig.12. (a) Side View (x - z plane) of the intruder in the bedroom 1; (b) original leg's position; (c) the new leg's position.

TABLE III. RADIUS RELATIVE TO EACH TRANSCEIVER (THIRD CASE).

Transceiver	Radius (meters)	Radius (cells)
TX1/RX1	1.53	51
TX2/RX1	1.38	46
TX3/RX1	1.71	57
TX4/RX1	1.02	34

As it can be seen in Fig.13, there is a slight difference between the signals. This small discrepancy is due to the fact that the intruder performed a minor movement (of 3 cm) of his leg. Despite this slight difference between the signatures, the system is able to properly locate the intruder.

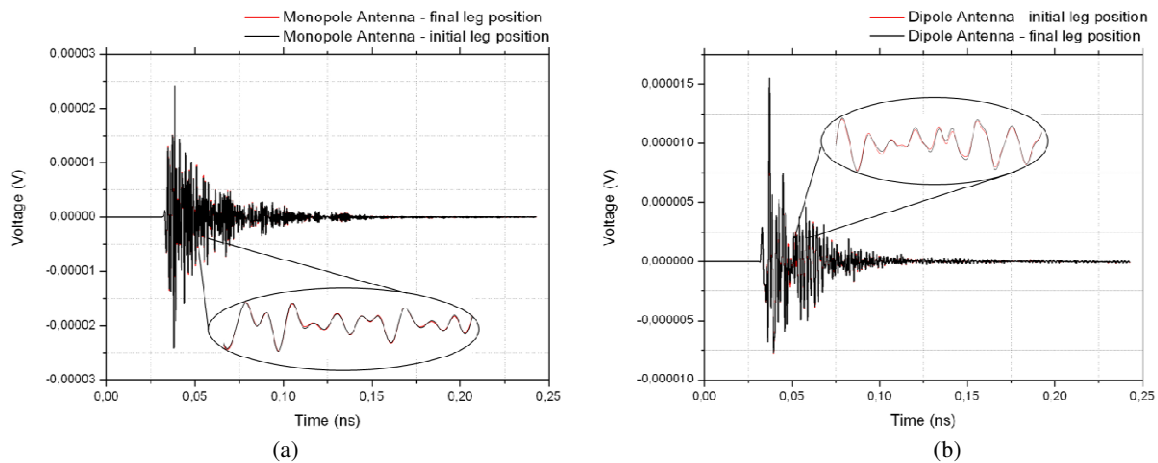


Fig.13. Signatures obtained at two receivers considering the initial and final positions of the intruder’s leg. In (a) Monopole Antenna and (b) Dipole Antenna.

In the fourth case, a second floor is added to the house considered in the previous simulations (Fig.14). In this case, all the transceiver antennas were kept on the first floor (same positions indicated by Fig.6) and half of quantity of the receivers was moved to the second floor. The intruder, who performs the same movement considered in the first case, was also placed at the second floor. In Fig.14, it is also depicted the smallest radius sphere of estimates (see Table IV). The region of space it encloses contains the intruder’s head. Here, only dipole antennas were employed.

TABLE IV. RADIUS RELATIVE TO EACH TRANSCIVER (FOURTH CASE).

Transceiver	Radius (meters)	Radius (cells)
TX1/RX1	1.71	57
TX2/RX1	0.87	29
TX3/RX1	1.23	41
TX4/RX1	0.48	16

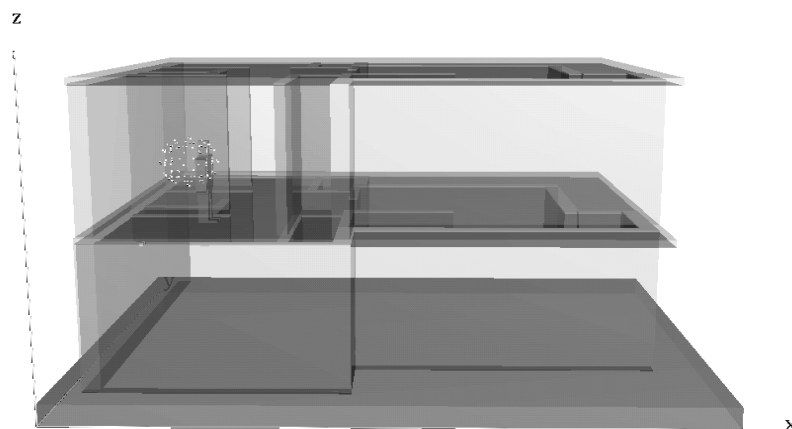


Fig.14. Side View (plane x-z) of the intruder in the second floor’s bedroom 1. Head movement is considered.

It is worth to mention that in real situations, the intruder and the other media, such as the soil and the walls, are not homogeneous materials. However, the electromagnetic signatures obtained due to the first pulse, which would take that into account, are used as reference signals. The signatures obtained due to the second pulse would also be affected by the non-homogeneous media. The latter is different from the former exclusively because of movement(s) inside the residence. This way, the proposed methodology is not dependent of this issue. For a given receiver, signatures obtained due the first and second pulses are identical to each other up to the moment in which the wave reflected by the intruder reaches the receiver. The oscillations observed in both signals are due the multipath components, which depend only on the residence elements, soil and on the radar system. The transient responses are also dependent on the intruder himself.

VI. CONCLUSION

This work presents a simple methodology, however effective, to perform the estimate of the position of an intruder in *tridimensional* environments. This way, a system of cooperative multistatic radars, operating with wideband pulses, was considered. The analysis of the problem was carried out by using the FDTD method, associated to the UPML formulation. The estimate of the position is performed by using vectors in the tridimensional space for defining the radar's ellipsoids. The results show that the proposed methodology is effective, since it can estimate the position of the intruder (target) in indoor environments, even if a slight movement is executed by him. The system can detect his presence and determine accurately his position in the environment. One can also notice that the system is adequate for two-floor buildings, in which it is necessary to consider receivers in both floors. For all the cases tested, the system correctly determined the room where the intruder was positioned and always the smaller sphere of estimates enclosed part of the man. It should be observed that in this paper particle swam optimization (PSO) was not employed (as it has been done in authors' previous 2D works) because it did not present good efficiency for the 3D case (minutes were necessary for obtaining the estimate). This way, the presented formulation provides the estimate in approximately three seconds (including the statistical analysis) when a 2 GHz processor is used. It is worth to mention that if more than one intruder is present inside the residence, two cases must be considered: 1) when the intruders are close to each other, they are detected as a single intruder, as long as the multiple estimates define a sphere which radius is comparable to the single intruder cases; 2) when the intruders are spread over the residence, the estimative spheres radii are considerable larger, due to the increase of the standard deviation. This way, it is possible to determine when more than one intruder is present. As a future work, experimental tests and a study regarding white noise (considering minimum transmitting power and detection threshold) are proposed.

REFERENCES

- [1] Taylor, J. D., *Ultra-Wideband Radar Technology*, Florida: CRC Press LLC, 2001.
- [2] Welch, T. B., Mulsselman, R. L., Emessiene, B. A., Gift, P. D., *et al*, “The effects of the human body on UWB signal propagation in an indoor environment”, *IEEE Journal on Selected Areas in Commun.*, vol.20, N° 9, December, 2002.
- [3] Müller, F.C.B.F., Farias, R.G., Sobrinho, C.L.S.S., Dmitriev, V., “FDTD Simulation of a Multistatic Radar Using Ultra-Wideband Pulses for Indoor Environments”, *Microwave and Optical Technology Letters*, Texas A&M University, College, v. 45, n. 5, p. 430-434, 2005.
- [4] Paolini, E., Giorgetti, A., Chiani, M., Minutolo, R., Montanari, M., “Localization Capability of Cooperative Anti-intruder Radar Systems”, *Journal on Advances in Signal Processing*, August, 2007.
- [5] Yee, K.S., “Numerical Solution of Initial Boundary Value Problems Involving Maxwell’s Equations in Isotropic Media,” *IEEE Trans. Antennas Propagat.*, vol. AP-14, pp. 302-307, May 1966.
- [6] Gedney, S. D., “An Anisotropic Perfectly Matched Layer – Absorbing Medium for the Truncation of FDTD Lattices”, *IEEE Trans. Antennas Propagat.*, vol. AP-44, No. 12, pp. 1630-1639, Dezembro, 1996.
- [7] Kondylis, G. D., “On Indoor Wireless Channel Characterization and the Design of Interference Aware Medium Access Control Protocols for Packet Switched Networks,” University of California, Los Angeles, 2000.
- [8] Oliveira, R. M. S., Sobrinho, C.L.S.S., Araújo, J. S., Farias, R. G., *Particle Swarm Optimization*, InTech Education and Publishing, Chapter 11, pp. 183-202, 2009.
- [9] Petroff A., and Withington, P., PulsOn Technology Overview, 2001, http://w.w.w.timedomain.com/files/downloads/techpapers/PulsONOverview7_01.pdf.
- [10] Gandhi, O. P., Lazzi, G., and Furse, C. M., Electromagnetic absorption in the human head and neck for mobile telephones at 835 and 1900 MHz, *IEEE Trans. Microwave Theory and Tech.*, vol. MTT-44, No. 10, October 1996.
- [11] Umashankar, K. R., “Calculation and experimental validation of induced currents on coupled wires in an arbitrary shaped cavity,” *IEEE Trans. Antennas and Propagation*, vol. 35, pp. 1248–1257, 1987.
- [12] Jackson, M. C., “The Geometry of Bistatic Radar System”, *IEE Proceedings*, vol. 133, no. 7, December, 1986.